JACS Au
AN OPEN ACCESS JOURNAL OF THE AMERICAN CHEMICAL SOCIETY
pubs.acs.org/jacsau
Letter

Side-Chain Length and Dispersity in ROMP Polymers with Pore-Generating Side Chains for Gas Separations

Francesco M. Benedetti,[†] You-Chi Mason Wu,[†] Sharon Lin,[†] Yuan He, Erica Flear, Kayla R. Storme, Chao Liu, Yanchuan Zhao, Timothy M. Swager, and Zachary P. Smith*

Cite This: JACS Au 2022, 2, 1610−1615
Read Online

ABSTRACT: Bottlebrush polymers with flexible backbones and rigid side chains have shown ultrahigh CO_2 permeability and plasticization resistance for membrane-based gas separations. To date, this class of polymers has only been studied with polydisperse side chains. Herein, we report gas transport properties of a methoxy (OMe) functionalized polymer synthesized via ring-opening metathesis polymerization (ROMP) with uniform side-chain lengths ranging from n = 2 to 5 repeat units to elucidate the role of both side-chain length and dispersity on gas transport properties and plasticization resistance. As side-chain length increased, both Brunauer−Emmett−Teller (BET) surface area and gas permeability increased with minimal losses in gas selectivity. Increased plasticization resistance was also observed with increasing side-chain length, which can be attributed to increased interchain rigidity from longer side chains. Controlling the side-chain length provides an effective strategy to rationally control and optimize the performance of ROMP polymers for CO_2-based gas separations.

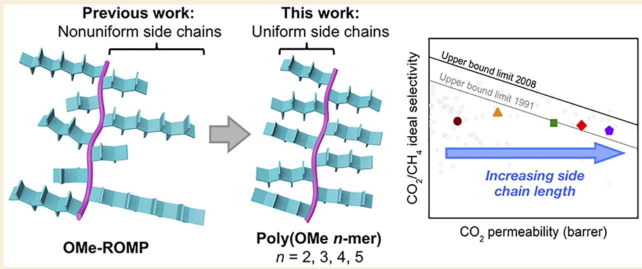

KEYWORDS: *ROMP, gas separations, bottlebrush polymers, porous polymers, side-chain length, plasticization resistance*

The use of membranes for gas separations is a promising alternative to traditional industrial separations due to their energy efficiency, low capital investment, and operational simplicity (i.e., no moving parts or phase changes).[1,2] In order to be suitable for scale-up and operation, such membranes must be solution-processable as well as highly permeable and selective.[3] Recently, polymers of intrinsic microporosity (PIMs) have emerged to define the state of the art in pure-gas performance due to their rigid and contorted backbones that lead to inefficient packing and concomitant pore generation, which results in very high gas permeabilities.[4−8] Since the discovery of PIMs, a range of design strategies (e.g., the incorporation of rigid groups such as iptycenes, Tröger's base and analogous motifs, fused norbornyl benzocyclobutene repeat units (CANALs), and polybenzoxazoles through thermally rearranged (TR) polymers) have been used to generate pores for improved separation performance.[9−18]

We recently introduced an alternative method to generate free volume using a "bottlebrush"-type polymer with a flexible poly(norbornene) backbone decorated with rigid, free-volume-generating side chains.[19,20] A variety of functionalities can be incorporated into the rigid macromonomers prior to their polymerization, allowing for the effects of these functionalities on polymer packing and gas transport properties to be studied. To that end, we investigated gas transport properties of two porous polymers generated via ring-opening metathesis polymerization (ROMP) with two different chemical substituents (CF_3-ROMP and OMe-ROMP) and found that CF_3-ROMP possessed ultrahigh CO_2 permeability (>21 000 barrer) and exceptional plasticization resistance (CO_2 plasticization pressure > 51 bar).[20] Although OMe-ROMP also displayed similar exceptional plasticization resistance, the CO_2 permeability was lower (∼2900 barrer).[20] These outstanding permeabilities, coupled with moderate selectivities of the major gas pairs considered, positioned CF_3-ROMP and OMe-ROMP across the separation performance upper bounds developed by Robeson for polymer materials.[20−22] The overall moderate selectivity of ROMP polymers compared to other PIMs with similar permeability was found to be related to limited diffusivity selectivity.[20] This finding is potentially related to the nonuniformity in side-chain length and the stereochemistry of the rigid side chains. Thus, we hypothesized that creating side chains of uniform length could potentially improve diffusivity selectivity, and consequently the permselectivity, in ROMP polymers.

In this study, we report gas transport properties of OMe-ROMP with uniform side chains ranging from n = 2 to 5 repeat

Received: April 7, 2022
Revised: May 23, 2022
Accepted: May 24, 2022
Published: July 7, 2022

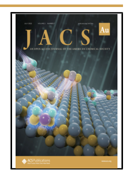

units (Figure 1), which we designate as poly(OMe *n*-mer)s. We found that increasing side-chain length (i.e., the value of *n*)

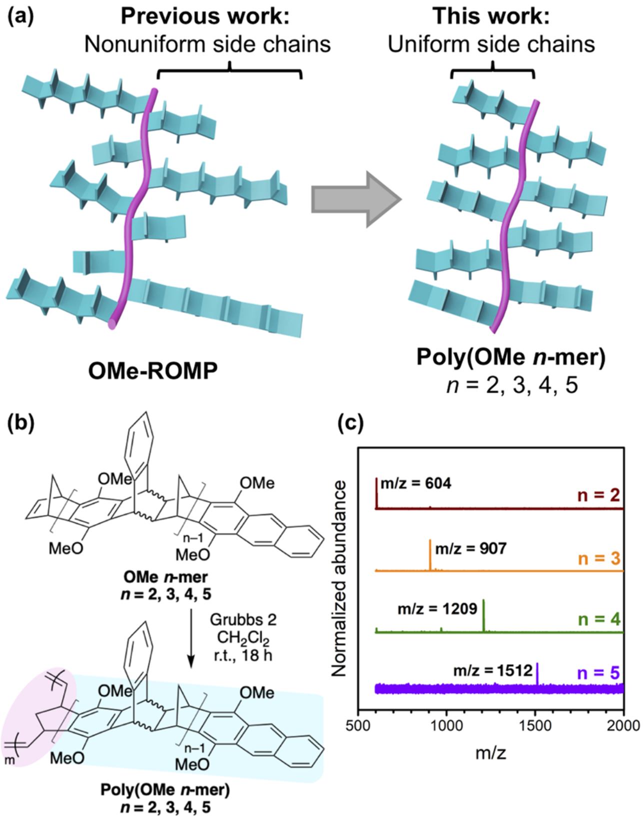

Figure 1. (a) Comparison of polymer structures between a previous study[20] and this study; (b) reaction conditions to polymerize OMe *n*-mers; (c) MALDI-TOF MS spectrum of each *n*-mer in this work.

led to increased pure-gas permeability and diffusion coefficients for all gases considered, with minimal loss in selectivity. Although we hypothesized that forming side chains of uniform length could improve selectivity, the dispersity of side-chain length in samples did not influence gas transport properties. For example, permeabilities, diffusivities, and selectivities of OMe-ROMP with polydisperse side chains (average n = 4.5) fell between those of poly(OMe 4-mer) and poly(OMe 5-mer). When measuring high-pressure pure-gas CO_2 permeation, increasing side-chain length correlated with increased plasticization pressures, suggesting that side-chain length presents a tunable parameter for enhancing plasticization resistance.

Figure 1a compares the architecture of the samples considered in our previous study[20] to those considered here. Poly(OMe *n*-mer)s were synthesized from their respective telechelic oligomers of uniform lengths (Figure 1b; see the Supporting Information for detailed procedure). These pure, but stereoirregular, OMe *n*-mers were obtained using silica gel column chromatography to separate the OMe-oligomer mixture obtained from Diels−Alder oligomerization. We successfully separated OMe *n*-mers of n = 1−5, whereas higher *n*-mers began to coelute (n = 1 corresponds to the unreacted monomer and was not further studied). We were unable to separate the fluorophilic CF_3 oligomers on silica gel, so they were not considered in this study. After isolation of the OMe *n*-mers, their identity and purity were confirmed by nuclear magnetic resonance (NMR) spectroscopy and matrix-assisted laser desorption/ionization−time-of-flight mass spectrometry (MALDI−TOF MS). The MALDI−TOF spectra, shown in Figure 1c, demonstrate expected m/z values with minimal impurities (see Table S1 for a comparison of expected and observed m/z values). In addition to MALDI, quantitative ^{1}H NMR integration ratios were also consistent for each OMe *n*-mer, confirming the assigned oligomer lengths (see Figure S1 and Table S2 for integration method and observed ratios). ROMP of the purified OMe *n*-mers using Grubbs second-generation catalyst provided the corresponding poly(OMe *n*-mer)s (Figure 1b). Monomer-to-initiator ratios ([M]/[I], based on molar concentrations) between 100 and 150 produced polymers of high molecular weights ($M_n \geq 75$ kDa; see Table S3) that were suitable for producing free-standing films via solution casting.

Brunauer−Emmett−Teller (BET) surface areas of poly(OMe 2-mer)−poly(OMe 5-mer) were obtained from N_2 adsorption isotherms (Figure S2) at 77 K and are shown in Figure 2 and Table S4. The BET surface areas show an

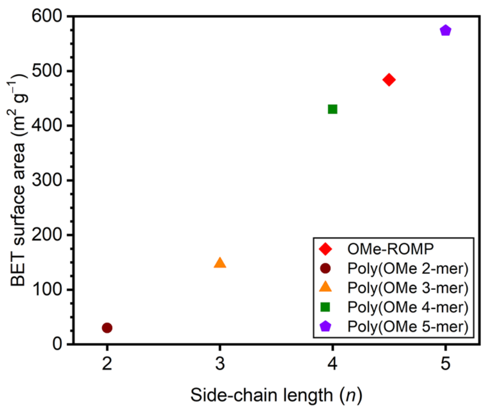

Figure 2. BET surface areas of poly(OMe 2-mer) through poly(OMe 5-mer), plus nonuniform OMe-ROMP (average n = 4.5).

increasing trend with increasing n, demonstrating the porogenic nature of the side chains. The BET surface area of OMe-ROMP falls between those of poly(OMe 4-mer) and poly(OMe 5-mer), which is consistent with an average n of 4.5 in OMe-ROMP as determined by NMR integration. The same N_2 adsorption data were used to determine the pore size distribution (PSD) of poly(OMe *n*-mer)s by means of nonlocal density functional theory (NLDFT) using the standard slit carbon model (Figure S2).[23] Interestingly, the model indicates that, with increasing n, average pore size decreases (e.g., with max at 20 Å for poly(OMe 2-mer) to 7.6 Å for poly(OMe 5-mer)). Additionally, the pore size distribution becomes narrower, and micropores are more abundant (i.e., incremental pore volume increases with increasing n).

In addition, the fractional free volume (FFV) of thermally treated films was determined using group contribution methods first developed by Bondi,[24] van Krevelen and Te Nijenhuis,[25] and Park and Paul[26] and updated by Wu et al.[27] Results are shown in Table S5 and Figure S3. Although there is a clear increase of FFV from n = 2 to 4, which suggests that the increasing rigidity from longer side chains leads to more frustrated chain packing, the FFV values for poly(OMe 4-mer) and poly(OMe 5-mer) are equivalent, regardless of the

https://doi.org/10.1021/jacsau.2c00219
JACS Au 2022, 2, 1610−1615

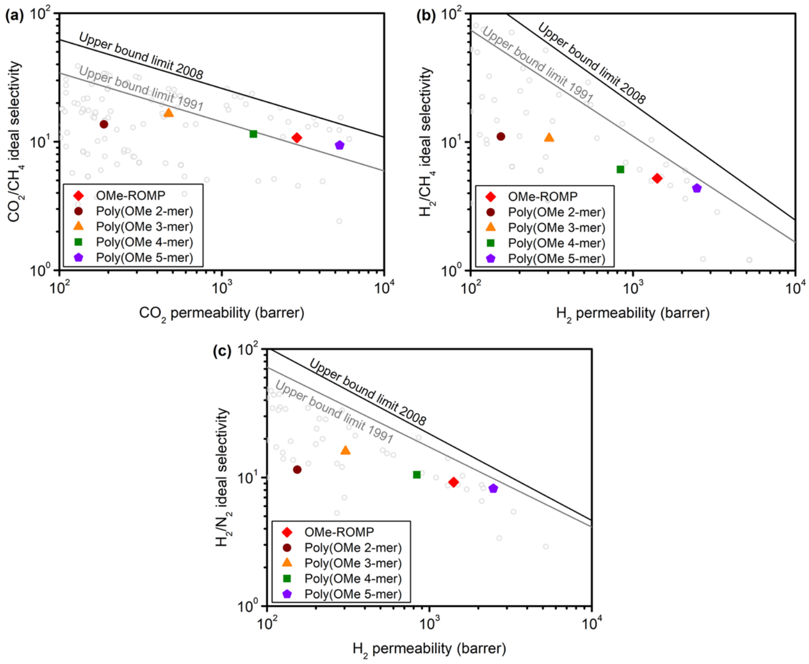

Figure 3. Robeson plots of alcohol-treated poly(OMe *n*-mer)s and OMe-ROMP for (a) CO_2/CH_4, (b) H_2/CH_4, and (c) H_2/N_2 gas pairs. Black and gray lines represent the 2008 and 1991 Robeson upper bounds, respectively.[21,22]

calculation method. Taken together, FFV and BET characterization support the interpretation that free volume and free volume distribution generally increase and narrow, respectively, with increasing side-chain length, but indirect probes such as gas permeation, which will be presented next, are required to clarify this physical picture.[28]

Pure-gas separation performance of all poly(OMe *n*-mer)s at ~1 bar upstream pressure and 35 °C are shown in Figure 3 and Table S6 for several gas pairs. Self-standing films were made by dissolving polymers in chloroform (3 wt %) and then cast into 50 mm flat-bottom glass dishes lined with Norton fluorinated ethylene propylene liners. After 4−5 days of evaporation at room temperature in a fume hood, free-standing films were generated. Before testing, films were soaked in methanol for 48 h, dried under ambient conditions for 24 h, and then degassed under full vacuum at 35 °C for 8 h. Since poly(OMe 2-mer) films were unable to withstand methanol treatment, ethanol treatment was used instead. Similar to methanol treatment, ethanol treatment has been shown to reset the thermal history of glassy polymers.[29−33]

Data for OMe-ROMP from our previous study is included in Figure 3 for comparison.[20] Similar to poly(OMe 2-mer), OMe-ROMP was treated with ethanol. For all samples tested, gas permeability increased as follows: $P(N_2) < P(CH_4) < P(O_2) < P(He) < P(H_2) < P(CO_2)$. As CO_2 is more permeable than H_2, this makes OMe-ROMP and poly(OMe *n*-mer)s reverse-selective membranes for this gas pair, indicating a strong sorption component to permeability.[34] As *n* increases, permeabilities for all gases increase, which correlates with increasing BET surface areas. Conversely, there is a weak negative correlation between selectivity and increasing side-chain length. Taken together, these findings indicate that side-chain length is a critical parameter for controlling permeability in the OMe-ROMP series, but there is only a limited effect on selectivity. In contrast with other PIMs, the bottlebrush design enables control of transport though side-chain synthesis. In addition, the upper bound performance of OMe-ROMP is in between that of poly(OMe 4-mer) and poly(OMe 5-mer), which is consistent with the average *n* of 4.5 for OMe-ROMP. Gas separation performance for thermally treated poly(OMe *n*-mer) samples, as well as data at different aging times, are shown in Figure S4 and Table S6.

In order to evaluate our original hypothesis that forming side chains of uniform length leads to increased diffusivity selectivity, we decoupled permeability, *P*, into diffusion, *D*, and sorption, *S*, coefficients using the sorption−diffusion model ($P = DS$).[35] Diffusion coefficients were determined using the time-lag method ($D = l^2/6\theta$), where *l* is the film thickness and θ is the time lag.[36] Since the time lags of He and H_2 were outside of the resolution of our permeation system (1−2 s), *D* and *S* are not reported for these gases. Tabulated diffusion and sorption coefficients for all samples in this study can be found in Table S6.

The effect of *n* on diffusion coefficients for O_2 is shown in Figure 4a for both thermally treated and methanol-treated samples. Analogous plots for N_2, CH_4, and CO_2 are shown in Figure S5a−c. For the four gases considered, as *n* increases, diffusivity increases in an exponential manner. As FFV generally increased with increasing *n* (Figure S3 and Table S5), this finding is in agreement with free volume theory, which states that the logarithm of diffusion (log*D*) is a linear function of 1/FFV.[37−40] For each gas, diffusion is lower in thermally treated samples compared to samples treated with methanol. This finding relates to methanol dilation of the membrane that leads to increased free volume.[30,41−45] The slopes of the semilog plots for thermally treated samples for each gas remain largely invariant, indicating that the change in diffusivity with respect to *n* is similar across all gases considered (Figures 4a and S5). However, for methanol-treated samples, the slopes of the semilog diffusivity plots increase ((0.38 ± 0.03) O_2 < (0.42 ± 0.03) CO_2 < (0.47 ± 0.07) N_2 < (0.53 ± 0.06) CH_4) in accordance with the effective diameter of the gas ((3.44 Å) O_2 < (3.63 Å) CO_2 ~ (3.66 Å) N_2 < (3.81 Å) CH_4). This result indicates that

https://doi.org/10.1021/jacsau.2c00219
JACS Au 2022, 2, 1610−1615

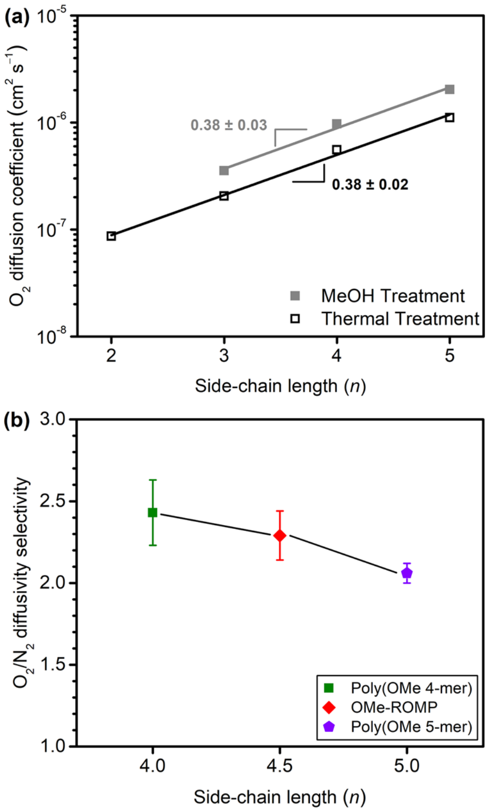

Figure 4. (a) O_2 diffusion coefficient for both thermally- and methanol-treated poly(OMe n-mer) samples versus side-chain length (n). Slopes and errors, determined using linear regression and χ^2 analysis, were calculated using the Origin 9.1 fitting tool. (b) O_2/N_2 diffusivity selectivity for n = 4 and n = 5 uniform poly(OMe n-mer) and nonuniform OMe-ROMP with average n = 4.5.

methanol-treated samples have a higher average FFV and a free volume distribution that more easily accommodates larger molecules with increasing side-chain length.[42,44] Table S7 reports diffusivity selectivity of OMe-ROMPs for a number of gas pairs, showing that diffusivity selectivity decreases with n and that uniformity of side chains has no effect on this trend. This data can be visualized in Figure 4b for O_2/N_2 and Figure S5d for other gas pairs.

Given the plasticization resistance of ROMPs,[20] methanol-treated poly(OMe n-mer)s were subjected to CO_2 pressures as high as 51 bar at 35 °C (Figure 5). The hysteresis induced by conditioning samples at 51 bar of CO_2 is also shown in Figures 5 and S6. Data for OMe-ROMP from our previous publication is included for comparison. Although poly(OMe 4-mer) and poly(OMe 5-mer) show excellent plasticization resistance similar to OMe-ROMP (CO_2 plasticization pressure >51 bar), poly(OMe 3-mer) exhibits a plasticization pressure of ~10 bar. For the poly(OMe 2-mer) film, the plasticization test was conducted on a thermally treated sample due to the mechanical fragility of the ethanol-treated sample, resulting in a plasticization pressure of ~15 bar. With increasing n, a decrease in hysteresis behavior was observed. For example, permeability at ~30 bar was ~18% higher upon depressurization for poly(OMe 5-mer), whereas OMe-ROMP exhibited a difference of 26% and poly(OMe 2-mer) of 67% under the same conditions (Figure S6). We previously hypothesized that large interchain cohesive energy present in ROMPs contributed to plasticization resistance.[20] Our results in this study indicate that higher n leads to stronger interchain cohesive energy and greater interchain rigidity. Detailed mixed-gas studies to deepen an understanding on the plasticization resistance of ROMPs will be the subject of a future publication.

In conclusion, we have polymerized discrete OMe oligomers to make bottlebrush polymers with uniform side-chain lengths of n = 2−5 to study the effects of n on gas transport. BET and permeability measurements indicated that both surface area and gas permeability increase as n increases. Although diffusivity increased exponentially as n increased, there was

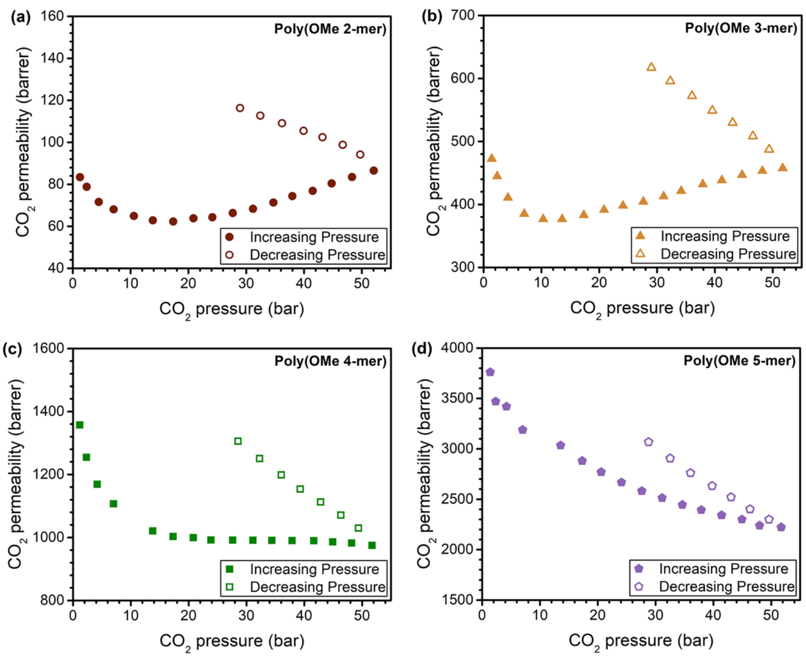

Figure 5. High-pressure pure-gas CO_2 permeability experiments conducted on (a) poly(OMe 2-mer), (b) poly(OMe 3-mer), (c) poly(OMe 4-mer), and (d) poly(OMe 5-mer). Note that poly(OMe 2-mer) was treated with ethanol while other samples were treated with methanol.

https://doi.org/10.1021/jacsau.2c00219
JACS Au 2022, 2, 1610−1615

not an appreciable effect on selectivity. Moreover, we found that uniform side-chain lengths did not lead to improved diffusivity selectivity as was originally hypothesized. CO_2 plasticization pressures increased with increasing n, suggesting that the exceptional stability of ROMPs is attributed to the inclusion of long, rigid side chains. Longer side chains than what have been studied here could further improve property sets such as permeability and plasticization resistance.

■ ASSOCIATED CONTENT

Supporting Information

The Supporting Information is available free of charge at https://pubs.acs.org/doi/10.1021/jacsau.2c00219.

Materials; synthetic procedures; characterization (silica gel chromatography, NMR spectroscopy, SEC, MALDI-TOF MS, BET surface area); molecular weights of poly(OMe n-mers) considered; BET surface areas, N_2 adsorption isotherms, and PSDs; film fabrication, treatment, and gas permeation measurement procedures; density, van der Waals volumes, and FFV of poly(OMe n-mer)s; pure-gas permeability, diffusion, and sorption coefficients for poly(OMe n-mer)s; Robeson plots of poly(OMe n-mer)s, OMe-ROMP, and CF_3-ROMP for CO_2/CH_4, H_2/CH_4, and H_2/N_2 gas pairs; diffusion coefficients versus side-chain length for N_2, CH_4, and CO_2; diffusivity selectivity versus side-chain length; hysteresis induced by conditioning of poly(OMe n-mer)s at 51 bar CO_2 (PDF)

■ AUTHOR INFORMATION

Corresponding Author

Zachary P. Smith − *Department of Chemical Engineering, Massachusetts Institute of Technology, Cambridge, Massachusetts 02139, United States;* orcid.org/0000-0002-9630-5890; Email: zpsmith@mit.edu

Authors

Francesco M. Benedetti − *Department of Chemical Engineering, Massachusetts Institute of Technology, Cambridge, Massachusetts 02139, United States;* orcid.org/0000-0002-2621-6649

You-Chi Mason Wu − *Department of Chemistry, Massachusetts Institute of Technology, Cambridge, Massachusetts 02139, United States;* orcid.org/0000-0002-6585-7908

Sharon Lin − *Department of Chemical Engineering, Massachusetts Institute of Technology, Cambridge, Massachusetts 02139, United States*

Yuan He − *Department of Chemistry, Massachusetts Institute of Technology, Cambridge, Massachusetts 02139, United States*

Erica Flear − *Department of Chemistry, Massachusetts Institute of Technology, Cambridge, Massachusetts 02139, United States*

Kayla R. Storme − *Department of Chemistry, Massachusetts Institute of Technology, Cambridge, Massachusetts 02139, United States*

Chao Liu − *Key Laboratory of Organofluorine Chemistry, Shanghai Institute of Organic Chemistry, Chinese Academy of Sciences, Shanghai 200032, China*

Yanchuan Zhao − *Department of Chemistry, Massachusetts Institute of Technology, Cambridge, Massachusetts 02139, United States; Key Laboratory of Organofluorine Chemistry, Shanghai Institute of Organic Chemistry, Chinese Academy of Sciences, Shanghai 200032, China;* orcid.org/0000-0002-2903-4218

Timothy M. Swager − *Department of Chemistry, Massachusetts Institute of Technology, Cambridge, Massachusetts 02139, United States;* orcid.org/0000-0002-3577-0510

Complete contact information is available at: https://pubs.acs.org/10.1021/jacsau.2c00219

Author Contributions

†F.M.B., Y.-C.M.W., and S.L. contributed equally to this work and are cofirst authors.

Notes

The authors declare no competing financial interest.

■ ACKNOWLEDGMENTS

This work was supported by the U.S. Department of Energy, Office of Science, Office of Basic Energy Sciences, Separation Science program under Award Number DE-SC0019087 and National Science Foundation DMR-1809740. F.M.B. gratefully acknowledges the funding and support provided by ExxonMobil Research and Engineering Company through the MIT Energy Initiative. F.M.B. and S.L. gratefully acknowledge the funding and support provided by the MIT Deshpande Center for Technological Innovation. The authors would like to thank the members of the Smith Lab at the Massachusetts Institute of Technology for useful discussions.

■ REFERENCES

(1) Galizia, M.; Chi, W. S.; Smith, Z. P.; Merkel, T. C.; Baker, R. W.; Freeman, B. D. 50th Anniversary Perspective: Polymers and Mixed Matrix Membranes for Gas and Vapor Separation: A Review and Prospective Opportunities. *Macromolecules* **2017**, *50* (20), 7809−7843.

(2) Koros, W. J.; Zhang, C. Materials for Next-Generation Molecularly Selective Synthetic Membranes. *Nat. Mater.* **2017**, *16* (3), 289−297.

(3) Sanders, D. F.; Smith, Z. P.; Guo, R.; Robeson, L. M.; McGrath, J. E.; Paul, D. R.; Freeman, B. D. Energy-Efficient Polymeric Gas Separation Membranes for a Sustainable Future: A Review. *Polymer* **2013**, *54* (18), 4729−4761.

(4) McKeown, N. B.; Budd, P. M. Polymers of Intrinsic Microporosity (PIMs): Organic Materials for Membrane Separations, Heterogeneous Catalysis and Hydrogen Storage. *Chem. Soc. Rev.* **2006**, *35* (8), 675−683.

(5) Rose, I.; Bezzu, C. G.; Carta, M.; Comesaña-Gándara, B.; Lasseuguette, E.; Ferrari, M. C.; Bernardo, P.; Clarizia, G.; Fuoco, A.; Jansen, J. C.; Hart, K. E.; Liyana-Arachchi, T. P.; Colina, C. M.; McKeown, N. B. Polymer Ultrapermeability from the Inefficient Packing of 2D Chains. *Nat. Mater.* **2017**, *16* (9), 932−937.

(6) Budd, P. M.; Makhseed, S. M.; Ghanem, B. S.; Msayib, K. J.; Tattershall, C. E.; McKeown, N. B. Microporous Polymeric Materials. *Mater. Today* **2004**, *7* (4), 40−46.

(7) Budd, P. M.; Ghanem, B. S.; Makhseed, S.; McKeown, N. B.; Msayib, K. J.; Tattershall, C. E. Polymers of Intrinsic Microporosity (PIMs): Robust, Solution-Processable, Organic Nanoporous Materials. *Chem. Commun.* **2004**, *4* (2), 230.

(8) Li, P.; Chung, T. S.; Paul, D. R. Gas Sorption and Permeation in PIM-1. *J. Membr. Sci.* **2013**, *432*, 50−57.

(9) Long, T. M.; Swager, T. M. Molecular Design of Free Volume as a Route to Low-κ Dielectric Materials. *J. Am. Chem. Soc.* **2003**, *125* (46), 14113−14119.

(10) Carta, M.; Croad, M.; Malpass-Evans, R.; Jansen, J. C.; Bernardo, P.; Clarizia, G.; Friess, K.; Lanč, M.; McKeown, N. B. Triptycene Induced Enhancement of Membrane Gas Selectivity for Microporous Tröger's Base Polymers. *Adv. Mater.* **2014**, *26* (21), 3526−3531.

(11) Carta, M.; Malpass-Evans, R.; Croad, M.; Rogan, Y.; Jansen, J. C.; Bernardo, P.; Bazzarelli, F.; McKeown, N. B. An Efficient Polymer Molecular Sieve for Membrane Gas Separations. *Science* **2013**, *339* (6117), 303−307.

(12) Luo, S.; Liu, Q.; Zhang, B.; Wiegand, J. R.; Freeman, B. D.; Guo, R. Pentiptycene-Based Polyimides with Hierarchically Controlled Molecular Cavity Architecture for Efficient Membrane Gas Separation. *J. Membr. Sci.* **2015**, *480*, 20−30.

(13) Corrado, T.; Guo, R. Macromolecular Design Strategies toward Tailoring Free Volume in Glassy Polymers for High Performance Gas Separation Membranes. *Mol. Syst. Des. Eng.* **2020**, *5* (1), 22−48.

(14) Wang, Y.; Ghanem, B. S.; Han, Y.; Pinnau, I. Facile Synthesis and Gas Transport Properties of Hünlich's Base-Derived Intrinsically Microporous Polyimides. *Polymer* **2020**, *201*, 122619.

(15) Smith, Z. P.; Hernández, G.; Gleason, K. L.; Anand, A.; Doherty, C. M.; Konstas, K.; Alvarez, C.; Hill, A. J.; Lozano, A. E.; Paul, D. R.; Freeman, B. D. Effect of Polymer Structure on Gas Transport Properties of Selected Aromatic Polyimides, Polyamides and TR Polymers. *J. Membr. Sci.* **2015**, *493*, 766−781.

(16) Park, H. B.; Jung, C. H.; Lee, Y. M.; Hill, A. J.; Pas, S. J.; Mudie, S. T.; Van Wagner, E.; Freeman, B. D.; Cookson, D. J. Polymers with Cavities Tuned for Fast Selective Transport of Small Molecules and Ions. *Science* **2007**, *318* (5848), 254−258.

(17) Lai, H. W. H.; Benedetti, F. M.; Ahn, J. M.; Robinson, A. M.; Wang, Y.; Pinnau, I.; Smith, Z. P.; Xia, Y. Hydrocarbon Ladder Polymers with Ultrahigh Permselectivity for Membrane Gas Separations. *Science* **2022**, *375*, 1390−1392.

(18) Wiegand, J. R.; Smith, Z. P.; Liu, Q.; Patterson, C. T.; Freeman, B. D.; Guo, R. Synthesis and Characterization of Triptycene-Based Polyimides with Tunable High Fractional Free Volume for Gas Separation Membranes. *J. Mater. Chem. A* **2014**, *2* (33), 13309−13320.

(19) Zhao, Y.; He, Y.; Swager, T. M. Porous Organic Polymers via Ring Opening Metathesis Polymerization. *ACS Macro Lett.* **2018**, *7* (3), 300−304.

(20) He, Y.; Benedetti, F. M.; Lin, S.; Liu, C.; Zhao, Y.; Ye, H. Z.; Van Voorhis, T.; De Angelis, M. G.; Swager, T. M.; Smith, Z. P. Polymers with Side Chain Porosity for Ultrapermeable and Plasticization Resistant Materials for Gas Separations. *Adv. Mater.* **2019**, *31*, 1807871.

(21) Robeson, L. M. The Upper Bound Revisited. *J. Membr. Sci.* **2008**, *320* (1−2), 390−400.

(22) Robeson, L. M. Correlation of Separation Factor versus Permeability for Polymeric Membranes. *J. Membr. Sci.* **1991**, *62* (2), 165−185.

(23) Seaton, N. A.; Walton, J. P. R. B.; quirke, N. A New Analysis Method for the Determination of the Pore Size Distribution of Porous Carbons from Nitrogen Adsorption Measurements. *Carbon N. Y.* **1989**, *27* (6), 853−861.

(24) Bondi, A. Waals Volumes and Radii. *J. Phys. Chem.* **1964**, *68* (3), 441−451.

(25) van Krevelen, D. W.; Te Nijenhuis, K. *Properties of Polymers*; Elsevier, 2009.

(26) Park, J. Y.; Paul, D. R. Correlation and Prediction of Gas Permeability in Glassy Polymer Membrane Materials via a Modified Free Volume Based Group Contribution Method. *J. Membr. Sci.* **1997**, *125* (1), 23−39.

(27) Wu, A. X.; Lin, S.; Mizrahi Rodriguez, K.; Benedetti, F. M.; Joo, T.; Grosz, A. F.; Storme, K. R.; Roy, N.; Syar, D.; Smith, Z. P. Revisiting Group Contribution Theory for Estimating Fractional Free Volume of Microporous Polymer Membranes. *J. Membr. Sci.* **2021**, *636*, 119526.

(28) Horn, N. R. A Critical Review of Free Volume and Occupied Volume Calculation Methods. *J. Membr. Sci.* **2016**, *518*, 289−294.

(29) Mitra, T.; Bhavsar, R. S.; Adams, D. J.; Budd, P. M.; Cooper, A. I. PIM-1 Mixed Matrix Membranes for Gas Separations Using Cost-Effective Hypercrosslinked Nanoparticle Fillers. *Chem. Commun.* **2016**, *52* (32), 5581−5584.

(30) Mason, C. R.; Maynard-Atem, L.; Al-Harbi, N. M.; Budd, P. M.; Bernardo, P.; Bazzarelli, F.; Clarizia, G.; Jansen, J. C. Polymer of Intrinsic Microporosity Incorporating Thioamide Functionality: Preparation and Gas Transport Properties. *Macromolecules* **2011**, *44* (16), 6471−6479.

(31) Bhavsar, R. S.; Mitra, T.; Adams, D. J.; Cooper, A. I.; Budd, P. M. Ultrahigh-Permeance PIM-1 Based Thin Film Nanocomposite Membranes on PAN Supports for CO2 Separation. *J. Membr. Sci.* **2018**, *564*, 878−886.

(32) Bushell, A. F.; Attfield, M. P.; Mason, C. R.; Budd, P. M.; Yampolskii, Y.; Starannikova, L.; Rebrov, A.; Bazzarelli, F.; Bernardo, P.; Carolus Jansen, J.; Lanč, M.; Friess, K.; Shantarovich, V.; Gustov, V.; Isaeva, V. Gas Permeation Parameters of Mixed Matrix Membranes Based on the Polymer of Intrinsic Microporosity PIM-1 and the Zeolitic Imidazolate Framework ZIF-8. *J. Membr. Sci.* **2013**, *427*, 48−62.

(33) Starannikova, L. E.; Alentiev, A. Y.; Nikiforov, R. Y.; Ponomarev, I. I.; Blagodatskikh, I. V.; Nikolaev, A. Y.; Shantarovich, V. P.; Yampolskii, Y. P. Effects of Different Treatments of Films of PIM-1 on Its Gas Permeation Parameters and Free Volume. *Polymer* **2021**, *212*, 123271.

(34) Lau, C. H.; Li, P.; Li, F.; Chung, T. S.; Paul, D. R. Reverse-Selective Polymeric Membranes for Gas Separations. *Prog. Polym. Sci.* **2013**, *38* (5), 740−766.

(35) Wijmans, J. G.; Baker, R. W. The Solution-Diffusion Model: A Review. *J. Membr. Sci.* **1995**, *107* (1−2), 1−21.

(36) Frisch, H. L. The Time Lag in Diffusion. *J. Phys. Chem.* **1957**, *61* (1), 93−95.

(37) Matteucci, S.; Yampolskii, Y.; Freeman, B. D.; Pinnau, I. Transport of Gases and Vapors in Glassy and Rubbery Polymers. In *Materials Science of Membranes for Gas and Vapor Separation*; John Wiley & Sons, Ltd: Chichester, UK, 2006; pp 1−47.

(38) Thran, A.; Kroll, C.; Faupel, F. Correlation between Fractional Free Volume and Diffusivity of Gas Molecules in Glassy Polymers. *J. Polym. Sci., Part B: Polym. Phys.* **1999**, *37* (23), 3344−3358.

(39) Cohen, M. H.; Turnbull, D. Molecular Transport in Liquids and Glasses. *J. Chem. Phys.* **1959**, *31* (5), 1164−1169.

(40) Lin, H.; Freeman, B. D. Gas Permeation and Diffusion in Cross-Linked Poly(Ethylene Glycol Diacrylate). *Macromolecules* **2006**, *39* (10), 3568−3580.

(41) Seong, J. G.; Zhuang, Y.; Kim, S.; Do, Y. S.; Lee, W. H.; Guiver, M. D.; Lee, Y. M. Effect of Methanol Treatment on Gas Sorption and Transport Behavior of Intrinsically Microporous Polyimide Membranes Incorporating Tröger's Base. *J. Membr. Sci.* **2015**, *480*, 104−114.

(42) Budd, P. M.; McKeown, N. B.; Ghanem, B. S.; Msayib, K. J.; Fritsch, D.; Starannikova, L.; Belov, N.; Sanfirova, O.; Yampolskii, Y.; Shantarovich, V. Gas Permeation Parameters and Other Physicochemical Properties of a Polymer of Intrinsic Microporosity: Polybenzodioxane PIM-1. *J. Membr. Sci.* **2008**, *325* (2), 851−860.

(43) Rogan, Y.; Starannikova, L.; Ryzhikh, V.; Yampolskii, Y.; Bernardo, P.; Bazzarelli, F.; Jansen, C.; Mckeown, N. B. Synthesis and Gas Permeation Properties of Novel Spirobisindane-Based Polyimides of Intrinsic Microporosity. *Polym. Chem.* **2013**, *4*, 3813−3820.

(44) Jue, M. L.; McKay, C. S.; McCool, B. A.; Finn, M. G.; Lively, R. P. Effect of Nonsolvent Treatments on the Microstructure of PIM-1. *Macromolecules* **2015**, *48* (16), 5780−5790.

(45) Fuoco, A.; Comesaña-Gándara, B.; Longo, M.; Esposito, E.; Monteleone, M.; Rose, I.; Bezzu, C. G.; Carta, M.; McKeown, N. B.; Jansen, J. C. Temperature Dependence of Gas Permeation and Diffusion in Triptycene-Based Ultrapermeable Polymers of Intrinsic Microporosity. *ACS Appl. Mater. Interfaces* **2018**, *10* (42), 36475−36482.

https://doi.org/10.1021/jacsau.2c00219
JACS Au 2022, 2, 1610−1615